SECOND SEMI-ANNUAL PROGRESS REPORT

For the Period

1 April 1963 - 30 September 1963

STUDIES OF THE FUNDAMENTAL CHEMISTRY PROPERTIES AND BEHAVIOR OF FUEL CELLS

Submitted to:

National Aeronautics and Space Administration

(NASA Grant NsG 325)

[1963] refs OTS: [illegible]

(NASA CR-

Submitted by

Professor J. O'M. Bockris, Director

2

The Electrochemistry Laboratory

The University of Pennsylvania U.

Philadelphia 4, Pennsylvania

6907000

PROJECTS AND PERSONNEL ENGAGED IN THE RESEARCH

Principal Investigator	Dr. J. O'M. Bockris
Project Leaders	Dr. H. Wroblowa Dr. L. Nanis

Project	
Potentials of Zero Charge	S. Argade
Deactivation of Electrodes	D. Swinkels
Nature of Catalysts	Dr. A. Reddy
Mechanism of Electrocatalysis	Dr. H. Dahms
Studies of the Mechanism of Porous Electrodes	B. Cahan
Theory of the Double Layer	Dr. T. Anderson

TABLE OF CONTENTS

	Page
Potentials of Zero Charge	1
Deactivation of Catalysts: Adsorption	8
Nature of Catalysts	23
Mechanism of Electro-Catalysis	27
Studies of the Mechanism of Porous Electrodes	39
The Theory of Electric Double Layers	46

POTENTIALS OF ZERO CHARGE

INTRODUCTION

The potential of zero charge (PZC) is to be determined on a series of solid metals by at least three independent methods. The large discrepancies among literature values for PZC makes independent checking essential. The metals are: thallium, lead, nickel, palladium, platinum, silver, and copper. The solution must be fairly dilute in order for the successful application of the capacity method and 0.001 N and 0.01 N H_2SO_4 and perchloric acid have been selected in order to minimize specific adsorption.

1. Capacitance Method

The Wayne-Kerr B221 transformer ratio arm bridge and associated circuits have been thoroughly tested and calibrated using mercury in various solutions. An extremely high degree of precision has been attained and this apparatus yields unambiguous capacitance measurements, i.e. false frequency variations have been eliminated. This precision is necessary since frequency effects are expected due only to the physical structure of the solid electrodes. In addition to the bridge improvements detailed in a previous report[1], the sensitivity of null detection has been increased ten-fold by eliminating capacitive loading of the wave analyzer output through tuning of the oscilloscope input cable.

The PZC is discernible on the capacity-potential relation for dilute solutions. The C-V curve goes through a distinct minimum at the PZC. At the PZC the charge on the metal, q_m is zero so that rearrangement of the double layer structure occurs, influenced by first the compact Helmholtz layer and extending further into the diffuse layer. The rearrangement may be considered as a decrease in orienting effect due to surface charge and both the compact and diffuse double layers approach the random distribution of charge found in the bulk electrolyte i.e. the thickness of at least the diffuse layer decreases. Now the total capacitance of the double layer may be considered as being composed of capacitive contributions from the Helmholtz and diffuse layers in series. Thus, the total capacitance is represented by

$$\frac{1}{C_{total}} = \frac{1}{C_D} + \frac{1}{C_H} \tag{1}$$

where C_H and C_D are capacities of the Helmholtz and diffuse layers respectively.

Considering each component of the double layer as a parallel plate condenser, an effective decrease in spacing, as q_m decreases and goes to zero at the PZC, results in an increase of capacitance. In fact, C_H changes much less than that of the diffuse layer, since any specific adsorption and dipole components remain. Thus, by Eq. (1), the total capacitance tends to a minimum, i.e. towards C_H since C_D greatly increases.

The rigorous solution purification techniques of this Laboratory will be used in conjunction with small spheres of the appropriate solid metals. Surface cleaning will be accomplished by suitable combinations of cathodic and/or anodic pulsing. A maximum amount of C-V data will be obtained near to the PZC.

2. Moving Wire Method

A method similar to that described by Jakuszewski[4] will be used. Wires of each of the metals to be tested will be arranged to travel in and out of solution at a fixed rate. A potentiostat will be used to fix the potential of the wire in a starting position of just contacting the electrolyte. As the wire travels into the solution, charging of the double layer must occur in order to maintain a constant potential. This charging current goes to zero at the PZC and is of opposite sign on either side of the PZC. Now, the capacity per unit area is

$$C = \frac{dq}{\Phi} \qquad (2)$$

At potentials near the PZC, $dq = q - q_{PZC}$ and since $q_{PZC} = 0$,

$$dq = q = C_{\Phi} (\Phi - \Phi_{PZC}) \qquad (3)$$

and for any area A

$$q = C_{\Phi} A (\Phi - \Phi_{PZC}) \qquad (4)$$

since generally

$$dq = idt \qquad (5)$$

and from Eq. (4)

$$dq = C_{\Phi} (\Phi - \Phi_{PZC})\, dA \qquad (6)$$

then

$$i = C \frac{dA}{dt} (\Phi - \Phi_{PZC}) \qquad (7)$$

It may be seen from Eq. (7) that if the wire lowering speed is known, i.e. dA/dt is known, and the current is measured for a fixed potential, the capacity at this potential may be obtained and thus this method may be used to check values determined with the bridge method. Of greater significance is the condition $\Phi = \Phi_{PZC}$ for which the charging current is zero for any rate of area change.

For a C value of about 10 μF/cm^2 and for Φ within a few tens of millivolts of the PZC, a lowering rate of 1 mm/sec will require a charging current of the order of tenths of microamps. A potentiostat (Wenking) available in this Laboratory is deemed sufficient for the major instrumentation for the moving wire experiments. Wire specimens will be initially cleaned by reduction of surface oxides by purified hydrogen at sufficiently high temperature where feasible and also by cathodic-anodic pulsing. It should be noted that the wires may be introduced into the electrolyte very quickly after cleaning so that contamination problems are minimized. Also, surface roughness is an advantage since only the PZC and not capacity per unit area is the sought-for quantity, i.e. dA/dt is increased by the occurrence of roughness for any given geometrical area.

3. Organic Adsorption Method

A technique for evaluating the PZC has been devised in this Laboratory by Green and Dahms.[3] This consists in the measurement of adsorption of non-polar organic substance by radiotracer methods.[1] The principle of the method is as follows.

It has been shown[3] that the coverage θ of neutral organic molecules depends on the electrostatic field across the Helmholtz double layer. Thus, for the given potential drop, V_H, across this layer the value of θ is fixed for the given concentration of organic compound, C_o.

The value of V_H at constant φ_0 (metal-solution PD) changes with concentration of the supporting electrolyte owing to the changes in ψ'-potential at the outer Helmholtz layer, except at the point of zero charge, where $\psi^{PZC} = V_H^{PZC} = \chi$ (dipole potential), since there is no contribution of ionic charges to the PD. Under conditions of low coverage of non-polar organic substance and in electrolytes exhibiting little specific adsorption, χ is relatively independent of electrolyte concentration, and the field across the Helmholtz double layer is constant.

Thus potential dependent organic adsorption curves obtained using various concentrations of supporting electrolyte at constant C_0 should have a common point at the PZC, provided the PZC is not changed by adsorption of organic material (non-polar substance, low coverage), nor by specific adsorption of electrolyte anions (electrolytes containing ClO_4^- anions).

The method to be used for determining adsorption of radioactively tagged organic substance (tape-method) has been described in the previous report.[1] The total activity of C-14 labeled organic is measured from a thin electrolyte layer adhering to a plate which has been moved out of the electrolyte after an equilibrium period at constant potential. The step of actual metal surface area determination by the B.E.T. method may be omitted by changing electrolyte concentration for one given tape. Naphthalene will be used with the dilute perchloric and sulphuric acid solutions and the previously mentioned metals. Also, after exploratory runs, the entire nature of the adsorption-potential curve will be given a secondary emphasis in favor of repeated determinations at and near the equivalence point for adsorption (PZC). For this purpose, also, other electrolyte concentrations will be used in order to locate the PZC with some precision. In addition to 0.001 and 0.01 N electrolytes, 0.005 N and 0.05 N electrolytes will also be studied with constant concentration of naphthalene.

DEACTIVATION OF ELECTRODES: ADSORPTION

INTRODUCTION

The method and results of investigation of the adsorption of n-decylamine on Ni, Fe, Cu, Pb and Pt had been described in the previous report.

The observed phenomena are interpreted below.

DISCUSSION

The adsorption isotherms at the potential of maximum adsorption are shown in Figure 1. A limiting coverage less than a monolayer is approached in each case, except on Pt, where multilayer formation occurs. The shift in the adsorption maximum to more negative potentials as $\theta \rightarrow 1$ indicates that a monolayer of n-decylamine molecule with the amine group towards the metal is first formed. A second layer then adsorbs more easily on the hydrophobic surface formed by all the hydrocarbon chains extending into solution.

Free Energy of Adsorption - The adsorption of an organic substance at the metal-solution interface may be written:

$$\text{Org (sol)} + n\ H_2O\ \text{(ads)} \rightleftharpoons \text{Org (ads)} + n\ H_2O\ \text{(sol)} \qquad (1)$$

where n is assumed to be independent of coverage or charge on the electrode. The standard free energy for the above process referred to unit mole fraction of organic or water in solution and on the surface is

$$\Delta G_a^o = - RT \ln \frac{(X_{org,ads})\ (X^n_{w,sol})}{(X^n_{w,ads})\ (X_{org,sol})} \qquad (2)$$

For dilute solutions $X_{w,sol} = 1$ and $X_{org,sol} = C_{org}/55.4$. On the surface

$$X_{org,ads} = \frac{\Gamma_{org}}{\Gamma_{org} - \Gamma_w} \tag{3}$$

where Γ_{org} and Γ_w are the number of moles of organic material and water respectively per unit area. Using $\Gamma_{org} = \theta\, \Gamma_{max,org}$ and $\Gamma_{max,w} = n\, \Gamma_{max,org}$ we have

$$X_{org,ads} = \frac{\theta\, \Gamma_{max,org}}{\theta \Gamma_{max,org} + (1 - \theta) n \Gamma_{max,org}} = \frac{\theta}{\theta + n(1 - \theta)} \tag{4}$$

Similarly:

$$X_{w,ads} = \frac{n\ (1-\theta)}{\theta + n\ (1-\theta)} \tag{5}$$

Introducing Eqs. (4) and (5) into Eq. (2) we obtain:

$$\Delta G_a^o = -2.3\ RT\ \log \left[\frac{55.4}{C_{org}} \cdot \frac{\theta}{(1-\theta)^n} \cdot \frac{\left\{ \theta + n(1-\theta) \right\}^{n-1}}{n^n} \right] \tag{6}$$

The corresponding isotherm is:

$$\frac{\theta}{(1-\theta)^n} \quad \frac{\left\{ \theta + n\ (1-\theta) \right\}^{n-1}}{n^n} = \frac{C_{org}}{55.4}\ \exp\ \left(\frac{-\Delta G_a^o}{RT}\right) \tag{7}$$

When $n = 1$, Eq. (7) reduces to the familiar Langmuir equation.

The standard free energy of adsorption at the adsorption maximum extrapolated to zero coverage for each system is given in Table I.

In the case of copper the coverage becomes sufficiently high so that lateral interactions become significant. The apparent standard free energy of adsorption calculated using Eq. (6) then varies with coverage as shown in Figure 2.

TABLE I

QUANTITIES RELEVANT TO THE ADSORPTION OF n-DECYLAMINE ON SOLID METALS FROM 0.9 N $NaClO_4$, 0.1 N NaOH SOLUTION

	Roughness factor	E_m ($\theta \rightarrow 0$)	ΔG_a^o at E_m ($\theta \rightarrow 0$)
Ni	1.32	-0.7 volt	-6.8 kcal/mole
Fe	1.77	-0.7 volt	-6.6 kcal/mole
Cu	1.38	-0.9 volt	-7.3 kcal/mole
Pb	1.95	-1.0 volt	-6.2 kcal/mole
Pt	1.22	-0.4 volt	-7.4 kcal/mole

Components of the Standard Free Energy of Adsorption - Adsorption from solution is influenced by several interactions between the metal, the organic compound and the water both on the surface and in the bulk. To discuss these thermodynamically we will consider two cycles, one for the organic compound and one for the water.

Thermodynamic cycle for water:

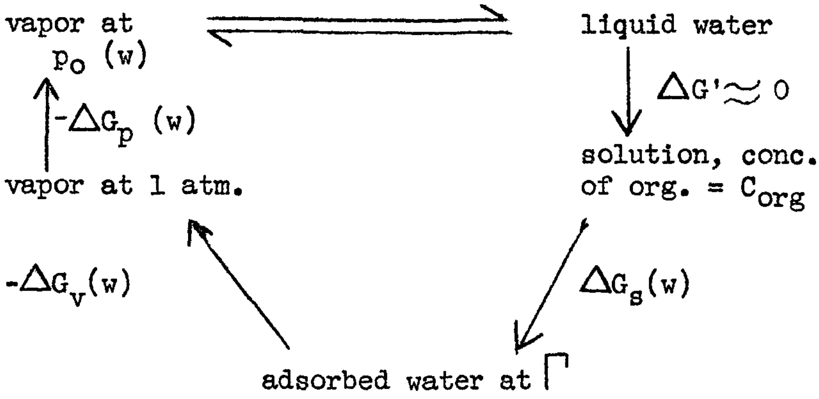
vapor at p_0 (w)
liquid water
$\Delta G' \approx 0$
solution, conc. of org. = C_{org}
$-\Delta G_p$ (w)
vapor at 1 atm.
$-\Delta G_v(w)$
$\Delta G_s(w)$
adsorbed water at Γ

For water:

$$\Delta G_s(w) = \Delta G_p(w) + \Delta G_v(w) \tag{8}$$

where $\Delta G_s(w)$ = free energy of adsorption of water from solution; $\Delta G_v(w)$ = free energy of adsorption of water from the vapor phase at 1 atm.; $\Delta G_p(w) = -RT \ln p_o(w)$ where $p_o(w)$ = vapor pressure of water at the temperature T.

Thermodynamic cycle for the organic material at the temperature T.

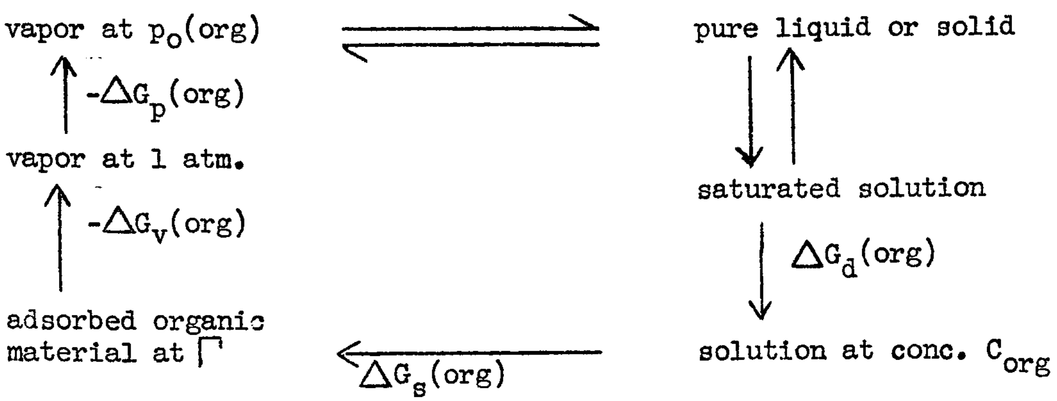
vapor at p_o(org)
$-\Delta G_p$(org)
vapor at 1 atm.
$-\Delta G_v$(org)
adsorbed organic material at Γ
pure liquid or solid
saturated solution
ΔG_d(org)
solution at conc. C_{org}
ΔG_s(org)

For the organic compound:

$$\Delta G_s(\text{org}) = -\Delta G_d(\text{org}) + \Delta G_p(\text{org}) + \Delta G_v(\text{org}) \tag{9}$$

where ΔG_s(org) = free energy of adsorption of the organic compound from solution at the concentration C_{org} and coverage Γ; ΔG_d(org) = free energy of dilution = $RT \ln \frac{C_{org}}{C_s}$; C_s = saturation concentration of organic; $\Delta G_p(\text{org}) = -RT \ln p_o(\text{org})$; p_o(org) = vapor pressure of the pure organic material at temperature T; ΔG_v(org) = free energy of adsorption of the organic compound from the vapor phase at 1 atm.

The standard free energy of adsorption from solution (ΔG_a^o) defined earlier, which is really the free energy of replacement of water at the interface, is then:

$$\Delta G^o_a = \Delta G^o_s(\text{org}) - n\Delta G^o_s(w) \qquad (10)$$

Using the standard state of unit mole fraction of organic material or water at the interface and in solution, we have:

$$\Delta G^o_a = -\Delta G^o_d(\text{org}) + \Delta G^o_p(\text{org}) - n\Delta G^o_p(w) + \Delta G^o_v(\text{org}) - n\Delta G^o_v(w) \qquad (11)$$

$$= -\,RT \ln \frac{C_s}{55.4} - RT \ln \frac{p_o(\text{org})}{p_o{}^n(w)} + \Delta G^o_v(\text{org}) - n\Delta G^o_v(w) \qquad (12)$$

The first two terms of Eq. (12) do not change with the metal and hence make the same contribution to ΔG^o_a for all metals. Eq. (12) also shows that at a given concentration the amount of adsorption increases as the solubility (C_s) of the adsorbate decreases.[4]

For the adsorption of n-decylamine at 25°C, $C_s = 5 \times 10^{-4}$ moles per liter[5] and $p_o(\text{org}) = 0.18\text{mm}$[6] and $p_o(w) = 23.8\text{mm}$.

Hence:

$$\Delta G^o_a = -6.80 + 2.74 + \Delta G^o_v(\text{org}) - n\Delta G^o_v(w) \qquad (13)$$

Thus, about half of the free energy of adsorption (cf. Table I) from solution is due to the escaping tendency from solution in the present case and the remainder arises from interactions with the metal (ΔG^o_v).

Dispersion Interaction between Water and Metals - The magnitude of ΔG^o_a and its relatively constant value for different metals suggests, that only physical forces are involved in the adsorption process. The dispersion interaction between an adsorbed molecule and a large plane metal surface is[7]

$$U_{Disp} = \frac{\pi \bar{N} C}{6R^3} \tag{14}$$

where $\bar{N}$ = number of metal atoms per cm^3; R = distance between the center of the molecule and the surface of the metal; C = constant for the system. Various expressions for C have been given[7] of which the following seems the most useful:

$$C = 6mc^2 \frac{\alpha_1 \alpha_2}{(\frac{\alpha_1}{\chi_1}) - (\frac{\alpha_2}{\chi_2})} \tag{15}$$

where m = mass of the electron = 9.11×10^{-28} gm; c = velocity of light = 3×10^{10} cm/sec; α_1, α_2 = polarizability of water and metal respectively; χ_1, χ_2 = diamagnetic susceptibility of water and metal. Experimental determinations of α and χ are not available for most metals. Pierotti and Halsey[8] have calculated α for copper and iron from the refractive indices of these metals. However, since they used refractive indices determined at different wavelengths for the two metals, and since the refractive index of a metal varies greatly with wavelength, the polarizabilities so obtained cannot be compared.

Since the molar refraction of conductors is approximately equal to the molar volume we have

$$\alpha = \frac{3R_o}{4\pi N} \quad \frac{3V_m}{4\pi N} \tag{16}$$

where R_o = molar refractivity; V_m = molar volume. Values of α calculated in this way are listed in Table II. Mercury is included, since its polarizability has been measured[9] and was found to be 5.05×10^{-24} cc.

This is 14% less than the value calculated from Eq. (16). All calculated values of α are therefore reduced by 14%, to give the corrected values in column 2, which are used in the dispersion calculation. The atomic diamagnetic susceptibility of the metals was calculated from

$$\chi = \frac{-e^2 a_o{}^{1/2}}{4mc^2} \sqrt{n\,\alpha} \qquad (17)$$

where e and m are the electronic charge and mass respectively; a_o = Bohr radius; n = number of electrons in the atom.

Agreement between χ (calc) and measured values[10] is fair for mercury and lead. Iron, nickel and platinum are paramagnetic, and the measured value for copper is low because of the presence of some paramagnetism.[14] Using α(corr) and χ(calc) for each metal and the measured values of α and χ for water the constant C was calculated for each system. Using Eq. (14) with R = 1.5 Å the dispersion interaction between water and the various metals was calculated. The values found vary little amongst the metals. This agrees well with the rather constant value of ΔG_a^o found for the different metals. The magnitude of U_{Disp} is very dependent on the value of R and hence may be as much as 50% in error but this would not affect the relative magnitude amongst the metals unless R varies with the metal.

Dispersion interactions between adsorbed organic molecules and the metal substrate can also be calculated. The values for different metals will vary in the same proportions as for water, but will be somewhat larger, since the polarizability of the organic molecule is greater than that of water. Hence a net heat of adsorption, which varies with

TABLE II

QUANTITIES RELEVANT TO THE DISPERSION INTERACTION BETWEEN WATER AND VARIOUS METALS

	α(calc) in cm^3	α(corr) in cm^3	χ(calc) in c.g.s.	χ (meas.) in c.g.s.	C (eq. 15)	U_{Disp} in kcal/mole
Ni	2.62×10^{-24}	2.25×10^{-24}	-1.68×10^{-29}	- - - - -	7.97×10^{-59}	16.2
Fe	2.82×10^{-24}	2.42×10^{-24}	-1.68×10^{-29}	- - - - -	8.16×10^{-59}	15.4
Cu	2.83×10^{-24}	2.43×10^{-24}	-1.78×10^{-29}	-0.87×10^{-29}	8.51×10^{-59}	16.0
Pb	7.24×10^{-24}	6.23×10^{-24}	-4.80×10^{-29}	-4.17×10^{-29}	22.53×10^{-59}	16.6
Pt	3.61×10^{-24}	3.10×10^{-24}	-3.30×10^{-29}	- - - - -	13.77×10^{-59}	20.3
Hg	5.87×10^{-24}	5.05×10^{-24}	-4.27×10^{-29}	-5.61×10^{-29}	19.48×10^{-59}	17.7
H_2O	- - - - -	1.45×10^{-24}	- - - - -	-2.16×10^{-29}	- - - - -	- -

the polarizability of the metal results. However, since n-decylamine molecules are not spherical, the dispersion calculation becomes more complex (cf. next section).

Lateral Attraction - When there is lateral attraction between adsorbed organic molecules the free energy of adsorption becomes more negative with increased coverage. This is clearly the case on copper (Figure 2).

The way in which the lateral interaction varies with coverage depends not only on the type of interaction (ion-dipole, dipole-dipole or dispersion) but also on the type of adsorption (localized or non-localized). In the case of localized adsorption the distance between the sites on the substrate is fixed and invariant with coverage, while the occupancy of the sites varies linearly as the coverage. Hence,[11] for localized adsorption the lateral interaction varies linearly with coverage.

For non-localized adsorption the distance between adsorbed molecules can vary continuously and specifically varies inversely as the square root of the coverage. If the interaction potential is of the form $U = {}^{B}/r^{n}$ then U varies as $\theta^{n/2}$ and hence, the variation in lateral interaction with coverage depends on the type of interaction. In general, for an interaction energy of the form ${}^{B}/r^{n}$ we have[12] for localized adsorption

$$\mu = B\,\theta \sum_{i=1}^{\infty} \frac{1}{r_i^{\,n}} \qquad (18)$$

for non-localized adsorption

$$\mu = B\left(\frac{n+2}{4}\right)\theta^{n/2}\sum_{i=1}^{\infty}\frac{1}{r_i^{\,n}} \tag{19}$$

where μ = chemical potential due to lateral interaction; r_i = distance between a given molecule and the i'th neighbor at full coverage. The summation is over all other molecules in the plane but converges rapidly when $n>2$. The summations were evaluated for n = 6 (dispersion) and n = 3 (dipole-dipole) for square and hexagonal arrays until the terms became less than 1% of the first term. In the case of n = 3 both parallel and anti-parallel arrays were considered. The results are shown in Table III.

The lateral interactions in the system n-decylamine on copper can now be calculated on the basis of four models:

1a. Localized adsorption, n-decylamine molecules rigid.

The n-decylamine molecules are treated as rigid rods, perpendicular to the surface with the amine group towards the solution and the dipole parallel to the surface (Figure 3).*

To calculate the lateral interaction due to dispersion forces, we must calculate the difference in the dispersion interaction between two n-decylamine molecules and between a n-decylamine molecule and a volume of water equal to the second n-decylamine molecule. Since it is the hydrocarbon chain, which is mainly concerned in the dispersive interaction, the polarizability (α) and molar volume (V_m) used for

---

* This model is chosen because of the lack of variation of the potential of the maximum of adsorption with coverage, i.e. zero $\Delta\chi$ due to the organic molecule.

TABLE III

$\sum \frac{1}{r_i^n}$ FOR VARIOUS SYSTEMS

	$n = 6$	$n = 3\ (\uparrow\uparrow)$	$n = 3\ (\uparrow\downarrow)$
Square array*	$\frac{4.64}{R^6}$	$\frac{7.8}{R^3}$	$\frac{2.68}{R^3}$
Hexagonal array	$\frac{6.42}{R^6}$	$\frac{9.24}{R^3}$	$\frac{4.5}{R^3}$

* R = distance between nearest neighbors at full coverage.

n-decylamine are taken as those of n-decane.[13] The polarizability is calculated from the refractive index of n-decane (n = 1.41).

$$\alpha\,(\text{org}) = \frac{3V_m}{4\pi N}\,\frac{(n^2 - 1)}{(n^2 + 2)} = 19.2 \times 10^{-24}\text{cc} \tag{20}$$

The dispersion interaction between two spherical molecules in a medium of dielectric constant ε is given by

$$U_{Disp} = \frac{-\,3h\nu_i\alpha_1\alpha_2}{4\,\varepsilon\,r^6} \tag{21}$$

Since the n-decylamine molecule is a long cylinder, we will divide it into four approximately spherical units and sum the interactions between each unit in one molecule and the four units of the other molecule (cf. Figure 3). The polarizability of each unit of the organic molecule is then $\alpha'(\text{org}) = \alpha(\text{org})/4 = 4.8 \times 10^{-24}$cc. For a volume of water equal to one of these units we have

$$\alpha'(w) = \frac{V_m \text{ (n-decane)}}{4\ V_m \text{ (water)}} \times \alpha(w) = 3.94 \times 10^{-24}\text{cc} \qquad (22)$$

Thus,

$$U_{Disp} = \frac{-3h\nu_i}{4\,\varepsilon}\,\alpha'(\text{org}) \left\{\alpha'(\text{org}) - \alpha'(w)\right\} \sum_{i=1}^{4} \sum_{j=1}^{4} \frac{1}{r_{ij}^{6}} \qquad (23)$$

where r_{ij} = distance between the i'th unit of one molecule and the j'th unit of the other (Figure 3); ν_i = a characteristic frequency for the electrons, which both for saturated hydrocarbons and for water is about 3×10^{15} sec^{-1}; h = Planck's constant; $\varepsilon \simeq n_{\infty}^{2} \simeq 1.9$.

Assuming a hexagonal array of adsorbed molecules the distance between nearest neighbors at full coverage is 4.9 Å.

Hence:

$$r_{ij} = \sqrt{(4.9)^2 + (\,|i-j| \times 3.66)^2} \qquad (24)$$

Using these values we find U_{Disp} = -0.19 kcal/mole and

$$\mu_{Disp} = 6.42\ \theta\ U_{Disp} = -1.22\ \theta \text{ kcal/mole} \qquad (25)$$

To calculate U_{Dipole} we have

$$U_{Dip} = \frac{-\mu^2}{\varepsilon r^3} \qquad (26)$$

where the dielectric constant ε varies with coverage. At low coverage the dipoles are separated by water molecules about 15 Å from the electrode surface, where the dielectric constant is that of bulk water ($\varepsilon \simeq 80$), while at full coverage the dipoles are separated by organic molecules (ε = 2). Assuming a linear combination of these at intermediate coverages, we have

$$\varepsilon = 80 - 78\,\theta \qquad (27)$$

Hence:

$$\mu_{Dip} = 4\,\theta\,U_{Dip} = \frac{-1.08\,\theta}{80 - 78\,\theta} \text{ kcal/mole} \qquad (28)$$

The total change in free energy of adsorption with coverage is equal to $\mu_{Disp} + \mu_{Dip}$ (curve 1a on Figure 2).

1b. Non-localized adsorption, n-decylamine molecules rigid.

In this case:

$$\mu_{Disp} = 6.42\left(\frac{n+2}{4}\right)\theta^3\,U_{Disp} = -2.44\,\theta^3 \text{ kcal/mole} \qquad (29)$$

$$\mu_{Dip} = 4.5\left(\frac{n+2}{4}\right)\theta^{3/2}\,U_{Dip} = \frac{-1.35\,\theta^{3/2}}{80 - 78\,\theta} \text{ kcal/mole} \qquad (30)$$

The curve marked (1b) in Figure 2 corresponds to this model.

2. Non-rigid molecules.

A long hydrocarbon chain can generally bend and twist in all directions. The fully stretched n-decylamine molecule is about 16 Å long. Hence, if the average hydrocarbon chain bends through 90° in the middle of the chain, then the dipoles of two molecules can pair up even at 10% coverage (average distance between adsorbed molecules 14.5 Å). At higher coverages, the hydrocarbon chain needs to bend less and less, until at full coverage the situation is almost the same as for rigid molecules. At low coverages the molecules can take up many orientations in which no dipole pair is formed, but since anti-parallel dipoles attract pairing is favored. It is difficult to calculate exactly the probability of pair formation at a given coverage. We will assume that the fraction of adsorbed molecules forming pairs is proportional to θ and that at full coverage all molecules are paired up. The attractive force between two anti-parallel dipoles 3 Å apart is $-\mu^2/r^3$, i.e., $U = 1.05$ kcal/mole. Hence $\mu_{\text{Dip pairs}} = \theta\, U = 1.05\, \theta$ kcal/mole.

To a first approximation the forming of pairs does not change the interaction between a given dipole and the remainder of the dipoles or the dispersion interaction. The contribution due to pairing is therefore added to the change in free energy calculated for models (1a) and (1b) to give the curves (2a) and (2b) in Figure 2.

The agreement with experiment is best for model 2b, i.e. non-localized adsorption and non-rigid molecules.

FIG. I Adsorption Isotherms for n- Decylamine

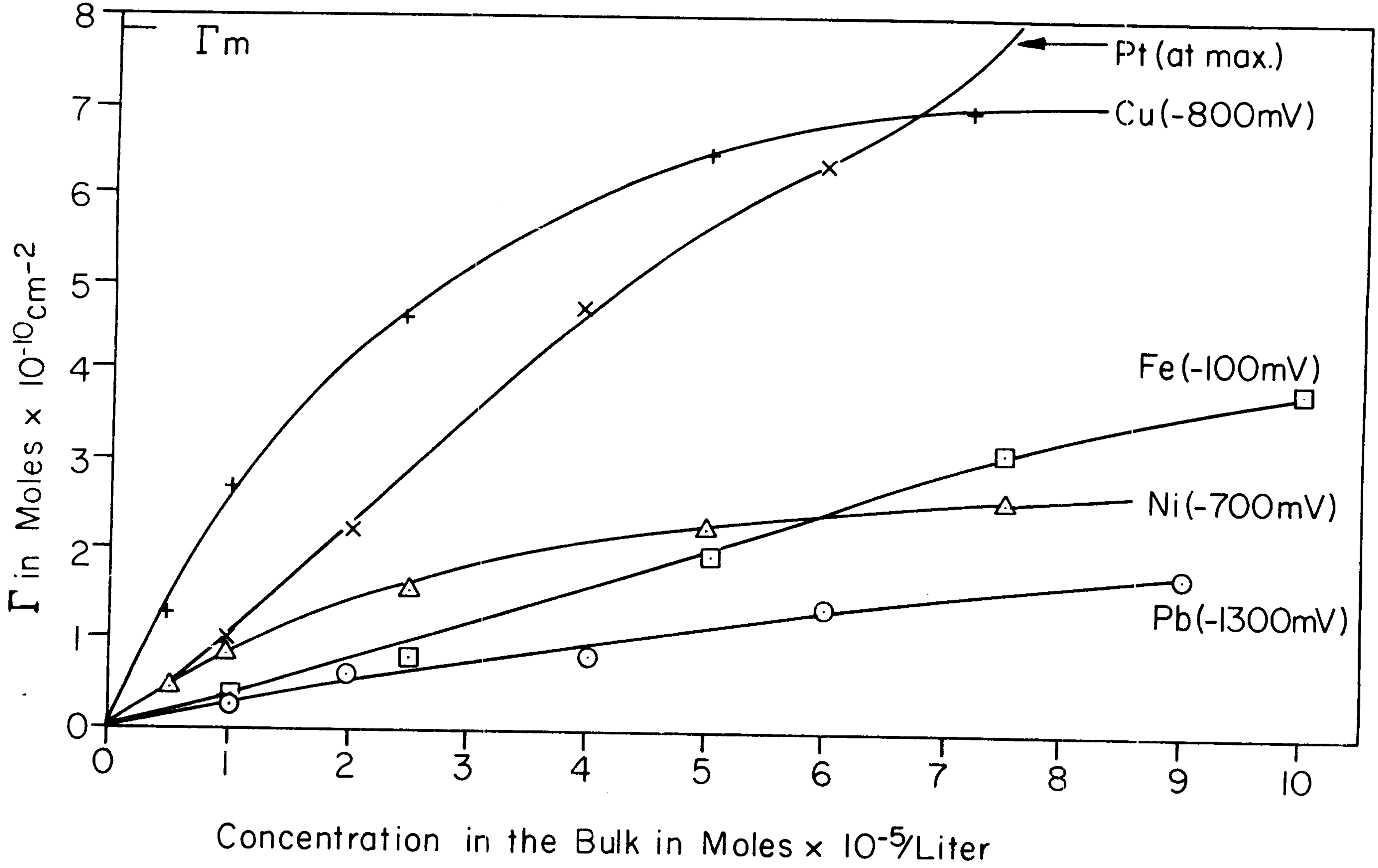

FIG.2 ΔG_a° for n-Decylamine on Copper as a Function of Coverage

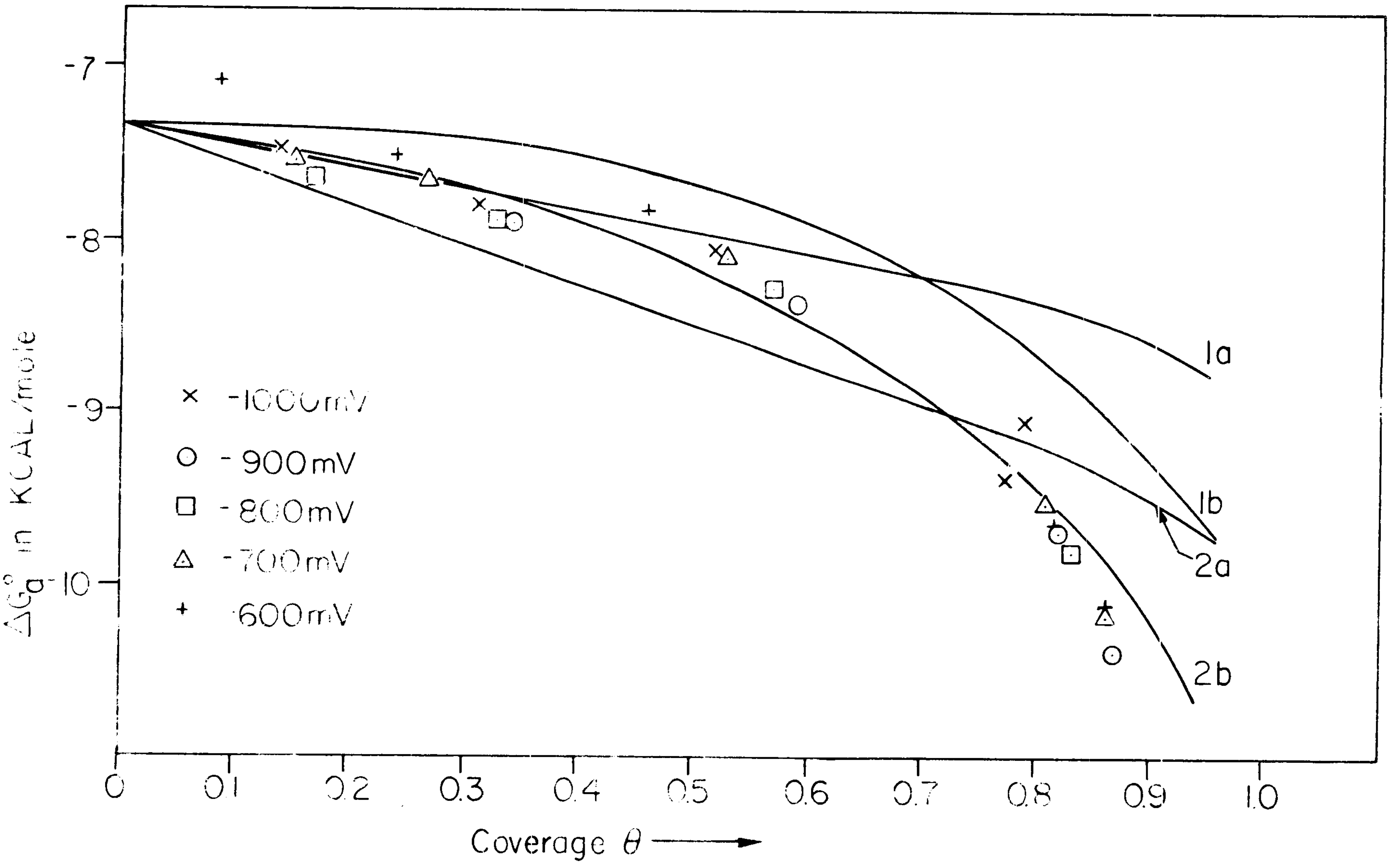

FIG. 3 MODELS FOR LATERAL INTERACTION CALCULATIONS BETWEEN n-DECYLAMINE MOLECULES

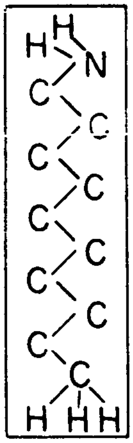

n-DECYLAMINE

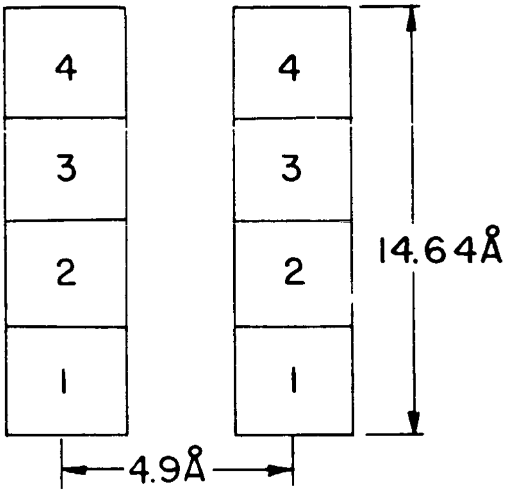

MODEL FOR DISPERSION CALCULATION

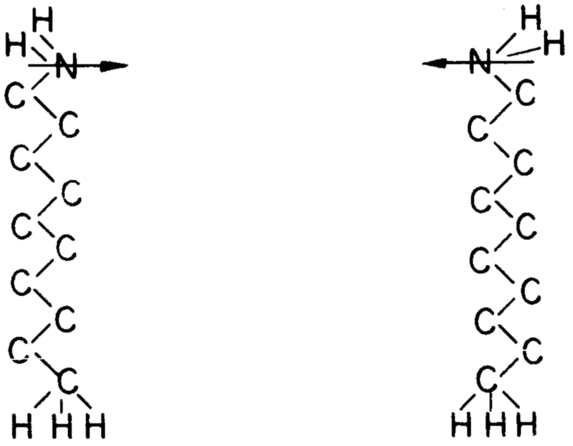

ODEL FOR DIPOLE - DIPOLE INTERACTION OF RIGID MOLECULES

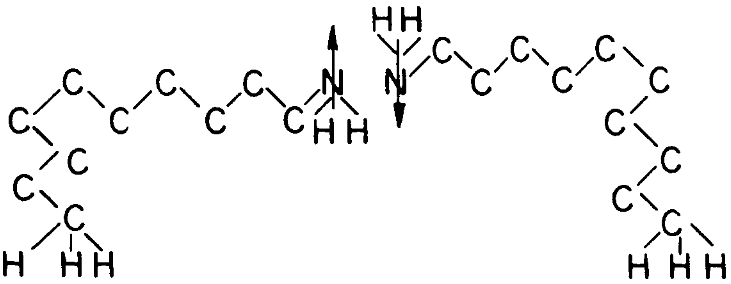

MODEL FOR DIPOLE PAIRS FORMED BY NON RIGID MOLECULES

NATURE OF CATALYSTS

INTRODUCTION

The preliminary experiments on the anodic formation of oxide films on platinum electrocatalysts have been continued utilizing *in situ* electrochemical and ellipsometric monitoring of the catalyst surface by (1) transient and (2) steady-state techniques.

(1) Method of Transients

The technique involves the following steps:

(a) Potentiostating the platinum catalyst at a potential of +0.300 v (vs N.H.E.) under which condition the platinum surface can be considered to be in its film-free optical reference state,

(b) Setting the optical components of the ellipsometer for "extinction"

(c) Switching off the potentiostat and simultaneously turning on a galvanostat

(d) Making simultaneous records of the potential-time and ellipsometer intensity-time traces on a Dual Channel Oscilloscope.

The type of transients observed are shown in Figure 4 from which it may be concluded that oxide formation commences at about 1 volt.

(2) Steady State Method

The potentiostat is used to hold the potential of the platinum electrode at various potentials and at each potential the optical components are set for extinction. For an angle of incidence on the window of the rectangular cell of 30° and an azimuth of the incident linearly polarized light of 45° to the plane of incidence, the extinction settings of the quarter-wave plate and analysis are set out in Table IV.

TABLE IV

Potential (volts vs N.H.E.)	Quarter-wave Plate	Analyzer
+0.34	338.23°	11.57°
+0.44	338.23°	11.57°
+0.54	338.23°	11.57°
+0.64	338.23°	11.57°
+0.74	338.23°	11.57°
+0.84	338.23°	11.57°
+0.94	338.23°	11.57°
+0.99	338.22°	11.54°
+1.04	338.57°	11.90°
+1.14	338.75°	12.11
+1.24	338.88°	12.27
+1.44	338.07°	12.50
+1.54	338.44°	12.88

From these settings, the relative phase retardation (Δ) and the relative amplitude diminution (χ) were calculated by standard formulae, and the potential dependence of these parameters is shown in Figure 5. It can be seen that there is no change in the optical constants of the platinum catalyst surface till a potential of about 1 volt is reached and since the optical constants at +0.34 v can be taken to correspond to a film-free surface, the results indicate that an oxide film is formed at about 1 volt.

The Drude-Tronstadt thin transparent film approximation was assumed in an attempt to compute the refraction index of the oxide. Negative values were obtained indicating that the refractive index is a complex quality which should be the case for a conducting film and since oxygen evolution occurs on the platinum catalyst, there can be no doubt that the oxide is an electronic conductor (or semiconductor).

Attempts are in progress to compute the refractive index and thickness of the film at various potentials by an electronic digital computer.

PLATINUM IN 0.1N H_2SO_4

FIG.4

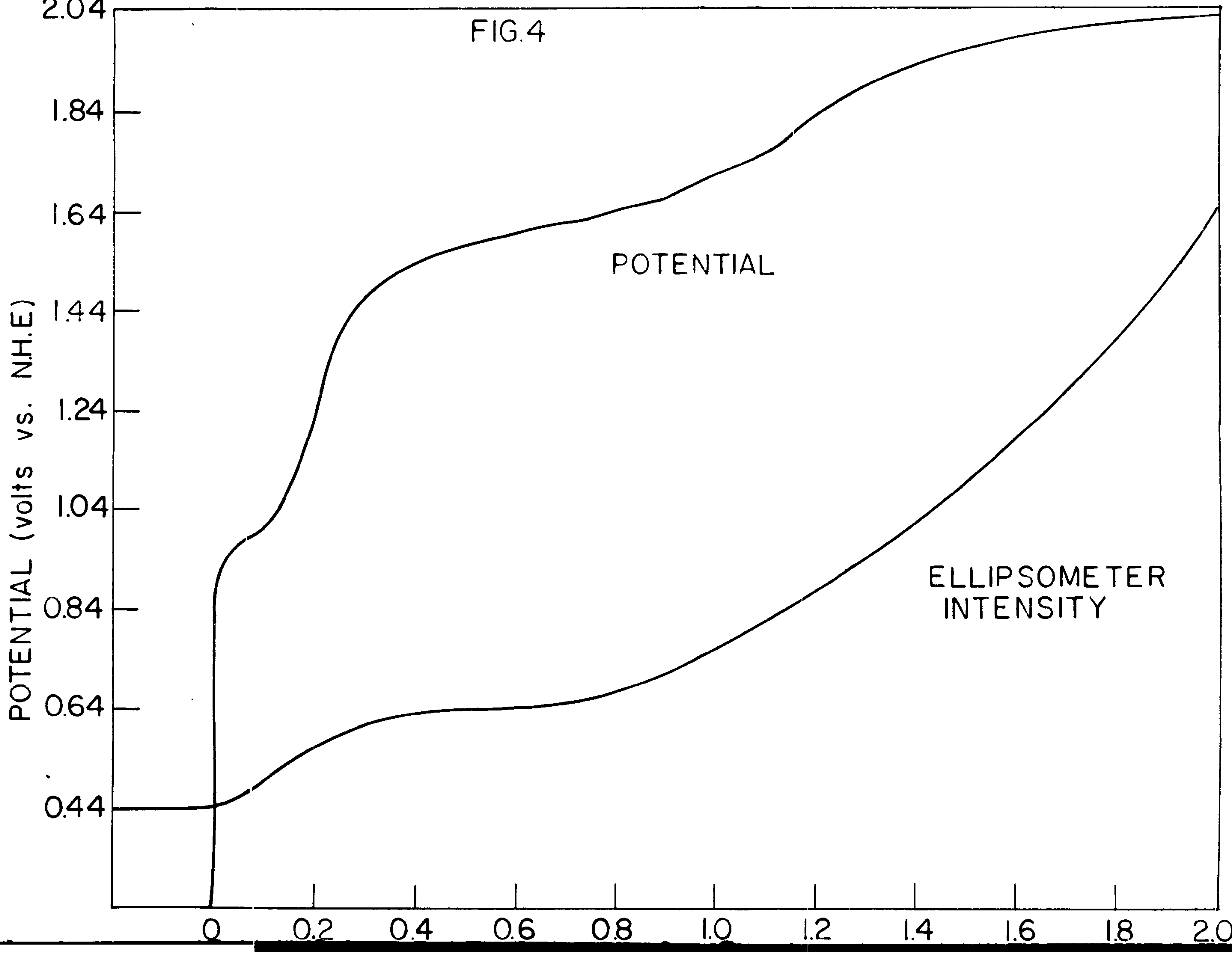

PLATINUM IN 0.1N H_2SO_4

FIG.5

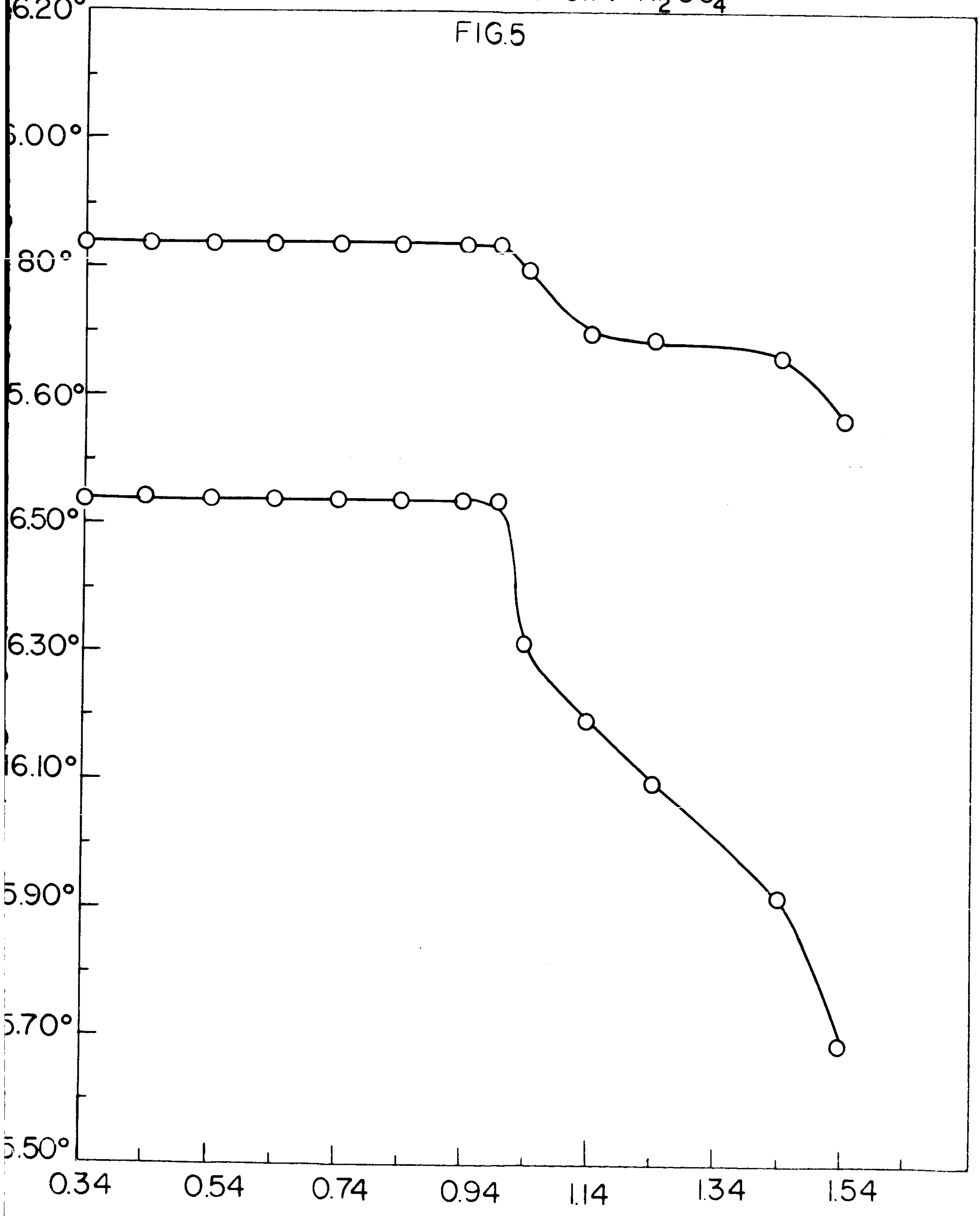

MECHANISM OF ELECTROCATALYSIS

INTRODUCTION

The experimental results reported in the First Semi Annual Report[1] have been interpreted.

DISCUSSION

1. Thermodynamics of the Reaction

The equilibrium potential can be easily calculated from the thermodynamic data of the reaction products.[4] For ethylene oxidation this value is found to be $E_o = 0.08$ at 80°C (hydrogen scale).

The rest potential of the system Me/ethylene appears to be a mixed potential.[15]

2. The "Chemical" Rate Constant

The rate of an activation-controlled reaction at an electrode is given by:[16]

$$i = nFkc \quad \exp\left[\frac{\alpha F\,(\Delta \mathcal{Y} + \phi_M - a)}{RT}\right] \qquad (1)$$

if there is no potential drop in the diffuse double layer and the rate of the back reaction is negligible. (n - number of electrons, F - Faraday, k - rate constant, α - transfer coefficient, $\Delta \mathcal{Y}$ - potential of electrode against standard hydrogen electrode, ϕ_M - electronic work function in eV, a - constant).

In order to bring out the "chemical" catalytic activity of the different metals we have to eliminate the influence of the applied electrical field. The electrical field across the interface can be written as:[17]

$$\Delta\varepsilon = \Delta\psi + \Delta\chi \qquad (2)$$

where $\Delta\varepsilon$ - potential difference against standard electrode (e.g., hydrogen electrode); $\Delta\psi$ - potential difference due to excess charges of metal; $\Delta\chi$ - potential difference due to orientation of dipoles.

It appears useful to define the "chemical" rate as the reaction rate at $\Delta\psi = 0$, i.e., at the potential of zero charge $\Delta\varepsilon = \Delta\varepsilon_{p.z.c.}$. As can be seen from Eq. (2), the potential of zero charge contains a dipole term. This term can be due to (a) the orientation of water dipoles at the interface and (b) the adsorption of the reactant and of intermediate reaction products on the electrode. The orientation of the water dipoles appears not to differ at the potential of zero charge greatly from metal to metal, since Frumkin[18] found the approximate relation:

$$\phi_{M_1} - \phi_{M_2} = \Delta\varepsilon^{o}_{M_1} - \Delta\varepsilon^{o}_{M_2} \qquad (3)$$

where ϕ_M - electronic work function; $\Delta\varepsilon^{o}_{M}$ - potential of zero charge.

The change of the $\Delta\chi$ potential with adsorption of the reactant and of the intermediates can be estimated from the change of the potential of zero charge on mercury with the adsorption of neutral[19] and charged[20] organic species: Typical values of this shift for full coverage of the electrode with neutral species are 0.1 - 0.2 V. Charged species could cause higher shifts, if present at sufficient concentrations (e.g., $\theta > 0.1$), which is improbable in the present system. Hence, the dipole term in Eq. (3) could cause an error of .1 - .2 V, which would lead to a maximal change of one power of ten in the "chemical" rate constant of Eq. (2) (β assumed = 0.5).

The definition of the "chemical" rate at $\Delta\Psi = 0$ may be considered as indicative (within these limits) of the reaction rate on the various surfaces free from double layer effects.

The factors determining the "chemical" rate constant at the interface metal/gas[21,22] are well known, e.g., they concern: (a) geometric factors which affect the activation energy of reactants;[23,24] (b) The electronic work function, which affects the heat of adsorption;[25] (c) The d-band structure influences the heat of adsorption (e.g., in the adsorption of hydrogen and ethylene).[26]

For catalysis at the metal-electrolyte interface, one has to take into account these factors, remembering that they can act both on the solute reactant and also upon the solvent reactant; for example, oxides will be formed in parallel reactions of the solvent with the metal and may participate either directly, or as inhibitors, in determining the rate of the reaction.

3. The Effect of the Applied Field

A change of the field across the double layer will have mainly two effects: It will (a) change the rate of any reaction step involving charge transfer; and (b) change the adsorption energy of the reactants, i.e. vary their concentration in the reaction zone.

The surface concentration of the organic reactant depends on the applied electric field. Analogous to the adsorption on mercury,[19] it has been found that there is a potential range of 0.2 - 0.4 V, where there is significant adsorption at the interface.[2,27] Roughly, the adsorption-potential relation is parabolic. Generally, there is a relation between the potential of zero charge and the potential of maximal adsorption (cf. adsorption on gold electrodes[2] and other metals.[27]), but exceptions occur on certain metals.[27]

In summary, the catalytic activity on an electrode is a resultant of the effects of the chemical rate constants and the double layer field effects, the degree of the effect of which is a function of the transfer coefficient, α. Hence, a low chemical rate constant on one metal can be compensated by a higher α on another.

4. Application to Present Reaction

a. Phenomenological

(1) The overall reaction.

The products of the overall reaction are given in Table V.

(2) The "chemical" rate constants.

These are given in Table V. The potentials of zero charge on which the calculations are based were determined experimentally only for Pt,[28,29] Au[2,30] and Pd.[29] The corresponding values for Ir and Rh were calculated from the empirical relation[31] between electronic work functions and potential of zero charge.

(3) The effect of the applied field.

The influence of the applied field on the reaction rate is given in Table V.

(4) The effect of pre-treatment.

The two pre-treatments[1] of the electrode do not cause essential differences in the reaction rates. The slight change in rate constants (but not in mechanism)[1] is probably due to roughness factor effects.

(5) Effect of oxide coverage on the reaction rate.

The oxide coverage affects the reaction rate for all metals in the same way: The electrode potential at which the oxide concentration exceeds a coverage of about 0.1 (Figure 20, ref. 1) corresponds to the potential (Figure 6) at which the Tafel line goes into a limiting region. The fact that an oxide coverage of 0.1 causes already a current decrease by a factor of 2 (compared to the extrapolated Tafel line) can be related to (a) geometric factors in the competitive adsorption of oxide and the organic species. Since C_2H_4 needs a four point attachment to the surface the blocking effect of small θ coverages will be great.[21] (b) The χ potential set up by the oxide. The dipole potential due to the oxide coverage will decrease the charge on the metal and, hence, lower the reaction rate.

b. Mechanistic Considerations

(1) Comparison of the metals.

The metals (Table V) fall into two groups of electrocatalytic activity: Group I (Pt, Ir, Rh) oxidizes the reactant quantitatively to CO_2 and shows approximately an identical Tafel slope (135 - 160 mV) and has the same pH dependence ($\sim$70 mV/pH$)_i$. Group II (Au, Pd) reveals imcomplete oxidation, has lower Tafel slopes and no pH dependence. Furthermore, the "chemical" rate constants of the Group I (Pt, Ir, Rh) metals tend to be higher.

The heats of sublimation show a clear difference for the metals Pt, Ir, Rh; and Au, Pd respectively. According to Pauling's equation, the bond strength for a partially covalent bond of the metal with an organic species is:

$$D(\text{org-Me}) = \frac{1}{2}\left\{D(\text{M-M}) + D(\text{org-org})\right\} + 23.06\,(X_{org} - X_M)^3 \qquad (4)$$

where D - bond energies between the respective species in kcal/mole; X - the electronegativities of the bond in Pauling units. Thus, for a given organic species the bond strength with metals of Group I (Pt, Rh, Ir) is higher by about 20 kcal than the bond strength with metals of Group II (Au, Pd).

The electronegativities of the metals[33] (Pd 2.0, Rh 2.1, Ir 2.1, Pt 2.1, Au 2.3) vary by 0.3 units. Taking the electronegativity of the organic species as 2.5 (value for C[34]) the electronegativity term changes by less than 5 kcal/mole among the metals examined. Thus, the bond strength between metals of Group I and metals of Group II differs by about 20 ± 5 kcal/mole. Consequently the bond metal-organic intermediate can be broken more easily with the Au, Pd metals: an incomplete oxidation would therefore be feasible, because intermediate oxidation products have a higher rate of desorption.

(2) Gold and Palladium

Considering the effect of ethylene partial pressure on the reaction rate (Figures 20,21, ref. 1) and the current potential dependence in the Tafel line region (Figures 15,16 ref. 1) the reaction scheme can be given by

$$A_{sol} \underset{k_{-1}}{\overset{k_1}{\rightleftharpoons}} A_{ads} \underset{k_{-2}}{\overset{k_2}{\rightleftharpoons}} X_1 + e;\; X_1 + B \xrightarrow[k_3]{rds} \ldots\ldots C \qquad (5)$$

where A_{sol}, A_{ads}, B represent stable chemical species in the solution

TABLE V

ETHYLENE OXIDATION AND CHARACTERISTIC PROPERTIES OF THE METALS

	Reaction product	"Chemical" reaction rate at p.z.c.* Amp/cm^2	pH dependence $(\frac{dE}{dpH})_i$	Tafel slope $(\frac{dE}{2.3d\log i})_{pH}$ mV	Lattice parameter Q [Å] (from 31)	Potential of zero charge $\Delta\mathcal{J}_{p.z.c.}$ (hydrogen scale)	Vacant d orbitals per atom (from32)	Heat of Sublimation L_S (kcal mole^{-1}) (from 22)
Platinum	CO_2	1×10^{-7}	70	160	c.f.c. 3.914	$+.30^{(18,19)}$	.55	135
Iridium	CO_2	1×10^{-11}	75	132	c.f.c. 3.823	$+0.05 \pm 100^{\neq}$	1.5	165
Rhodium	CO_2	5×10^{-11}	70	155	c.f.c. 3.794	$0.05 \pm 100^{\neq}$	1.5	138
Gold	no CO_2 aldehydes	1×10^{-11}	0	72	c.f.c. 4.070	$+.30^{(2,30)}$	0	84
Palladium	no CO_2 aldehydes	7×10^{-10}	0	80 - 110	c.f.c. 3.879	$+.25^{(29)}$	.55	91

* potential of zero charge (formerly: e.c.m.)

≠ calculated eq. (4) using electronic work functions.(31)

(excluding ions from water) and on the electrode, X_1 represents an intermediate. The current can be written as*

$$i = nFk_3 \frac{K_1 p_E}{1 + K_1 p_E} \cdot K_2 \, e^{VF/RT} \qquad (6)$$

where n - number of transferred electrons, $K_1 = \frac{k_1}{k_{-1}}$, $K_2 = \frac{k_2}{k_{-2}}$, p_E - pressure of ethylene; V - electrode potential.

This scheme gives rise to a b value of RT/F, its zero pH effect and (qualitatively, depending on the isotherm applied) the pressure dependence experimentally observed (Figures 18,19 ref. 1; Table V). To suggest a specific scheme is made difficult by the fact that the reaction goes to three products, the dominant of which is propionaldehyde. It seems possible that this is formed as a product from solution reactions with acetaldehyde, which might be regarded as the first product of the electrode reaction. It is difficult to find a reaction sequence which is consistent with the facts of Table V. The following type of mechanism obeys this criterion, though involves the assumption of a $C_2H_4^+$ intermediate. Evidence that reactions with this radical could be slow arises from its stabilization by solvation.

$$C_2H_{4\,sol} \xrightleftharpoons[k_{-1}]{k_1} C_2H_{4\,ads}$$

$$C_2H_4 \xrightleftharpoons[k_{-2}]{k_2} \overset{+}{C_2H_4}{}_{ads} + e$$

---

*This expression implicitly assumes a Langmuir isotherm with one-point attachment, whereas C_2H_4 is probably adsorbed with four-point attachment. However, no qualitative differences result in the interpretation of the pressure effect.

$$C_2H_4^+{}_{ads} + H_2O \xrightarrow[r.d.s.]{k_3} C_2H_4OH_{ads} + H^+$$

$$C_2H_4OH_{ads} \xrightarrow[fast]{k_4} C_2H_4O + H^+ + e$$

Then, the relatively greater chemical rate constant on Pd rather than Au may be roughly interpreted so: In the rate-determining reaction, the heats of activation will be determined primarily by the heats of adsorption of $C_2H_4^+$ and CH_3CHO; as also by the thermionic work function of the metal. Other factors which determine the heat of activation at the potential of zero charge are, for example, the heat of hydration of the proton and other factors which are independent of catalyst. Very roughly, one can now suppose that the heat of adsorption of $C_2H_4^+$ and the CH_3CHO do not greatly differ; for they will be made up mostly of the energies of two M-C bonds. Thus, the major difference resides in the work function: the faster reaction will occur in the metal which has the higher work function, and the expected ratio of chemical rate constants will be:

$$\frac{i_{Pd}}{i_{Au}} = e^{(\phi_{Pd} - \phi_{Au})\beta F/RT} \qquad (7)$$

The work function data for Pd and Au are poor.[31] The most probable are: Pd 4.9; Au 4.7. If these values are accepted, the difference in rates agrees fairly with that observed (expt.: $\frac{i_{Pd}}{i_{Au}} = 70$; theoret: $\frac{i_{Pd}}{i_{Au}} = 10^3$).

Similar remarks would apply to any mechanism of the oxidation of ethylene in which a stable chemical species is in equilibrium with an unstable one through a charge transfer reaction; and thereafter the unstable species goes to a stable one by a chemical (no net charge transfer) reaction.

(3) Platinum, Iridium, Rhodium

For platinum a substantial study of the mechanism of ethylene oxidation has been made by Weber and Green[35] (alkaline solution) and Wroblowa, Piersma and Bockris[36] (alkaline and acid solutions). Since Tafel slope, pH dependence and reaction products on Ir and Rh are identical to those on Pt (Table V), these considerations apply to these metals as well.

Rate-determining water discharge is deduced for the whole pH range.[36] All following reactions are in equilibrium and do not affect the overall reaction rate. Hence, the relative catalytic power depends upon factors which determine the rate of

$$H_2O \longrightarrow OH_{ads} + H^+ + e \qquad (8)$$

Of these, the work function and the heat of adsorption of reactant and product depend on the catalyst.

It is difficult to make an estimate concerning the difference in the heat of adsorption of H_2O and OH on these metals. OH is chemisorbed.[37] If water is chemisorbed,[38,39] then the bonding is likely to be between the metal and the two orbitals of oxygen, i.e., there is likely to be considerable compensation of any difference as both M-OH (in the final state) and M-OH_2 (in the initial state) would change in the same direction. Hence, the relative catalytic power is largely in terms of work function, i.e.:

$$\frac{k_{chem,Pt}}{k_{chem,Rh}} = e^{(\phi_{Pt} - \phi_{Rh})\beta F/RT} \qquad (9)$$

An analogous relation will hold for Ir. The work function data are fairly spread out. Taking the most probable value for Pt (5.3 eV) and Rh (4.9 - 5.1 eV) and Ir (4.9 - 5.0 eV) one obtains from Equation (9) $k_{chem,Pt} \cong 10^3 k_{chem,Rh} \cong 10^3 k_{chem,Ir}$. The experimental values give a factor of $k_{chem,Pt} = 2.10^3 k_{chem,Rh} = 10^4 k_{chem,Ir}$.

(4) Conclusions

In summary, the model arising from here is that on noble metals electrocatalysts there is a potential range in which C_2H_4 is adsorbed and its rate in the subsequent reaction depends primarily upon the relation of the potential for the adsorption range to the thermodynamic reversible potential for a given reaction. If two possibilities are near, e.g., $C_2H_4 \longrightarrow CO_2$ and $C_2H_4 \longrightarrow CH_2CHO$, then, which occurs depends on the relative binding of the intermediate radicals: the smaller this is, the less likely the reaction to go to completion. The final product, and path of reaction having been established by the factors mentioned, the relative catalytic properties of the "chemical" (or zero field standardized) rate constant is affected by one or two relatively simple properties such as work function or heat of adsorption of reaction and product. For the electrocatalysts studied here, these approaches are consistent with the facts.

FIG.6

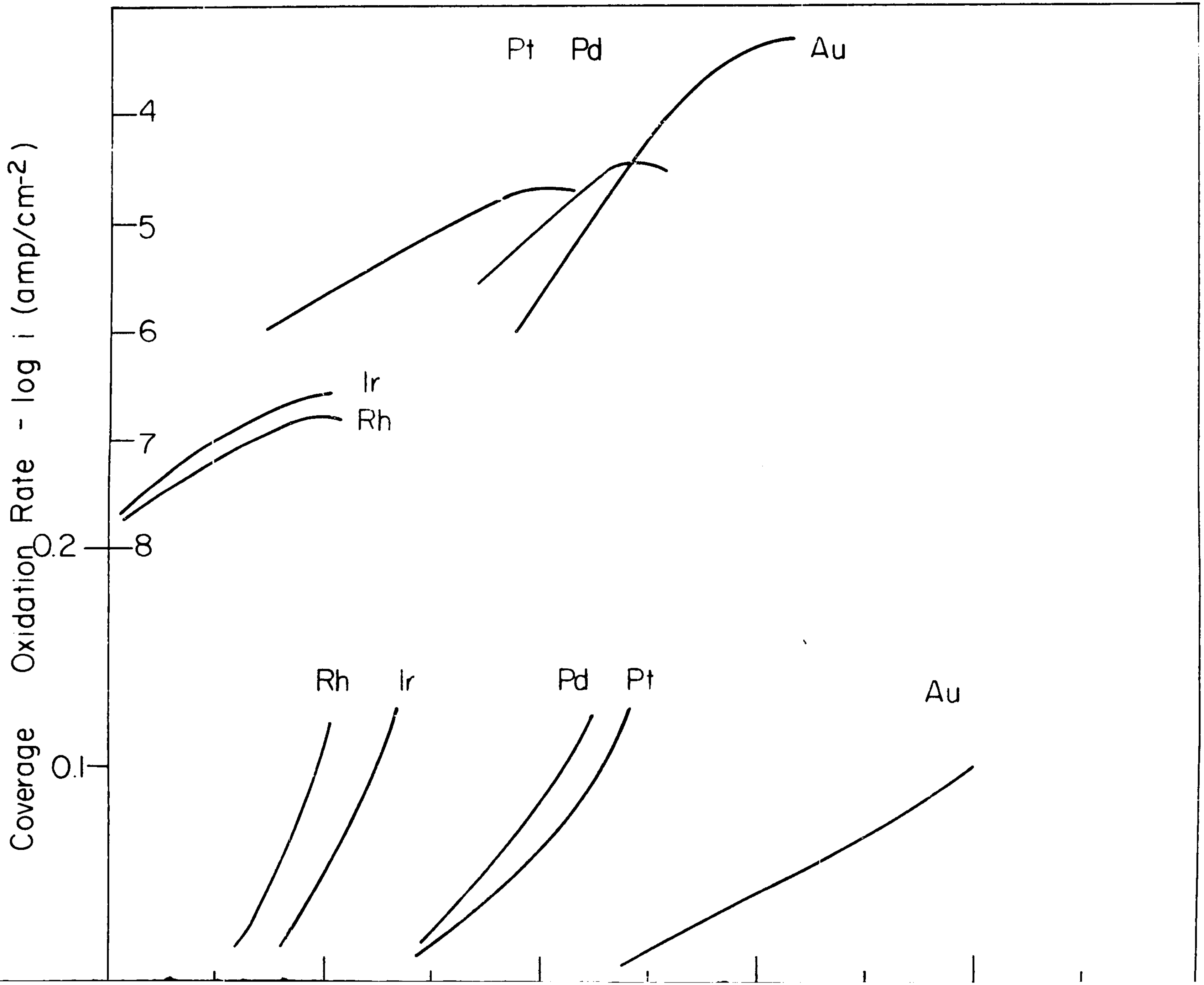
Pt
Pd
Au
-4
-5
-6
-7
0.2
-8
Ir
Rh
Oxidation Rate - log i (amp/cm-2)
Rh
Ir
Pd
Pt
Au
Coverage
0.1

STUDIES OF THE MECHANISM OF POROUS ELECTRODES

INTRODUCTION

The exact localization of the sites of reaction in a porous electrode structure is an extremely complex problem. The structure of the simplest of porous electrodes for actual fuel cell use is at best only poorly understood.

It is obvious, however, that in a highly porous electrode, usually chosen for its high surface area, most of the pores will be less than 10μ across. A more systematic study of extremely thin pores must therefore be made to evaluate the utilization of surface area, and minimize power losses in tortuous passages.

EXPERIMENTAL

The cell described in the last report has been constructed and is shown in Figure 8. The cell is mounted on a Vee-flat optical bench for rigidity of the micromanipulator support shown at the right. The adjustments "y" and "z" axes are hand-scraped light-duty machine mounts actuated by 1/4"-40 ground micrometer threads. These mounts can be set to a repeatability of better than .0002". The x-axis translation is accomplished by a micromanipulator with coarse and fine controls. The fine control has a resolution of 2.5 microns per div. and should provide resolution to 1.0μ. Connecting the top of the micromanipulator to the cell is the push-rod, coupled by a Teflon universal joint. The bearings are of polished stainless rod, press-fit in a Teflon block to provide smooth action and avoid backlash problems. The push-rod is connected rigidly to the piston in the cell and causes both translation and minute angular (vertical and horizontal) alignment. Because of the mechanical advantage involved, the alignment should be adjustable to within 0.00001 inches, or about 1/2 of a light fringe over the electrode surface.

The cell is shown at the left side of the illustration and in Figure 9. It consists of a block of Teflon FEP mounted rigidly in an aluminum frame. The front working surface has been machined to ± .001" over the entire surface. An optically flat (< 1/4 fringe) fused silica plate is mounted with a pressure plate (far left) against the working surface. This window allows inspection of the meniscus of the electrolyte, and the inside of the cell. The working electrode is made from a specially ground block of fused quartz visible in Figure 9. One surface of this block has been ground to within 1/4 fringe, has a sharp edge with roundness less than 5 microns, and no detectable chips in the central working area. The flat surface of the block is platinized and serves as the wall of the "pore".

The cell was constructed of FEP Teflon for the following reasons.

(1) Since FEP is a melt-processable resin, in contrast to the TFE, which must be sintered, the diffusion of gaseous impurities is markedly decreased.

(2) FEP does not undergo a phase transition near room temperature as does the TFE, and, consequently, much greater machining precision is possible. For example, the bore and piston for the moveable electrode has been machined to a tolerance of ± .001 inches in a 2" diameter.

Figure 10 is a magnified sketch of the cell in cross section and shows the model that will be used for calculations. The quartz window serves as a plane of symmetry between the real platinum electrode and its image. (The meniscus has been drawn flat, but in reality its shape will be affected by several controllable factors.) Affixed to the bottom of the cell is a micro-piston burette, whose volume can be varied to within 10^{-5} ml.

This model pore can thus be used to study a wide variety of experimental conditions since the pore width, and the depth of electrolyte penetration can be varied simultaneously. The surface can be studied in the "wetted" or "waterproofed" condition as electrolyte can be squeezed into or withdrawn at will from the pores. Since the electrode has an equivalent one-dimensional configuration, orders of magnitude more current can be drawn from it than from a cylindrical pore of equivalent diameter, with the further advantage that the meniscus height and shape can be viewed directly.

THEORETICAL CALCULATIONS

In contrast to the model of Will, in an extremely thin pore ($< 3\mu$) the meniscus shape is considerably modified. If the electrode material is wetted, the pore will fill completely by a wick action. If it is not wetted, the meniscus will be relatively flat with a sharp demarcation at the boundary.

In either case, it can be represented diagramatically as in Figure 11a. Here, the concentration gradient of the gas is in the same direction as the ion current, whereas in Will's model these fluxes are perpendicular, (Figure 11b).

With similar assumptions for boundary conditions, the two systems yield very different equations.

It is convenient to assume a flat pore of unit length, a separation "t", and a depth of penetration "ℓ" (cf. Fig. 11a). Further, assuming that activation control is absent, and that concentration polarization and IR drop are the only controlling factors, then,

$$C_x = C^o e^{-z\phi E} \qquad (1)$$

where C_x is the concentration of H_2 at a point $0 \leq x \leq \ell$ measured from the point where the capillary joins the bulk solution. C^o is the equilibrium concentration of H_2 assumed to exist at the gas electrolyte interface $x = \ell$, and $\phi = F/RT$. Differentiating, Eq. (1) yields

$$\frac{dC_x}{dx} = - z\phi C^o e^{-z\phi E} \frac{dE}{dx} \qquad (2)$$

(If t is small compared to ℓ, $dC/dy \cong 0$).

Since H_2 can only enter at the interface, and the pore is considered uniform, the total equivalent current, I_T, per unit length through a slice at $x = x$ is made up of two parts: (1) the unreacted dissolved gas, and the H^+ ions that have already reacted. Therefore

$$I_T - I_{ionic} = I_{diff}. \qquad (3)$$

or by Fick's law,

$$I_T - I_x = zFDt \frac{dC_x}{dx} \qquad (4)$$

Only the ionic component, I_x, will produce an IR drop in the electrolyte, i.e.

$$\frac{dE}{dx} = - \frac{I_x \rho}{t} \qquad (5)$$

where ρ is the solution resistivity.

Combining (4) and (5) gives

$$\frac{dE}{dx} = - \frac{I_T \rho}{t} + \rho \, zFD \frac{dC_x}{dx} \qquad (6)$$

and substituting (2) in (6) gives

$$\frac{dE}{dx} = - \frac{I_T \rho}{t} - \rho \, z\phi C^o \, zFD \, e^{-z\phi E} \frac{dE}{dx} \qquad (7)$$

Now, separating variables leads to

$$dE \, (1 + \rho \, zFD \, z\phi C^o \, e^{-z\phi E}) = - \frac{\rho I_T}{t} dx \qquad (8)$$

Integration of Eq. (8) gives

$$E - \rho \, zFDC^o \, e^{-z\phi E} = - \frac{\rho I_T x}{t} + C \qquad (9)$$

When $x = 0$, $E = E_a$ (E_a = the applied potential referred to the bulk solution),

$$E_a - \rho \, zFD \, C^o \, e^{-z\phi E_a} = C \qquad (10)$$

Substituting Eq. (10) in Eq. (9) gives

$$E_a - E + \rho \, zFD \, C^o \, (e^{-z\phi E} - e^{-z\phi E_a}) = \frac{\rho I_T x}{t} \qquad (11)$$

When $x = \ell$, $C_\ell = C^o$ and the anodic concentration overvoltage $E = 0$. Therefore

$$E_a + \rho \, zFD \, C^o \, (1 - e^{-z\phi E_a}) = \rho I_T \ell / t \qquad (12)$$

Solving Eq. (12) for I_T, substituting in Eq. (11), and rearranging terms, gives

$$\frac{x}{\ell} = \frac{(E_a - E) + \rho \, zFD \, C^o \, (e^{-z\phi E} - e^{-z\phi E_a})}{E_a + \rho \, zFD \, C^o \, (1 - e^{-z\phi E_a})} \qquad (13)$$

Since the local current density i, is, by definition, $i = - \frac{dI_x}{dx}$

$$i = - \frac{d}{dx} \left(zFDt \frac{dC_x}{dx}\right) \qquad (14)$$

$$i = \frac{d}{dx} \left[zFDt \ z\phi \ C^o \ e^{-z\phi E} \frac{dE}{dx} \right] \qquad (15)$$

Substituting from Eq. (7) in Eq. (15) with differentiation gives

$$i = zFDt \ z\phi C^o \ z\phi \left[E_a + \rho \, zFD \ C^o(1 - e^{-z\phi E_a}) \right] (1 + \rho zFDC^o \ z\phi \ e^{-z\phi E}) \frac{dE}{dx} \qquad (16)$$

or $$i = - \frac{{I_T}^2 \rho}{t} \frac{z^3 \phi^2 \rho \, FDC^o \ e^{-z\phi E}}{(1 + \rho \, zFD \ z\phi C^o \ e^{-z\phi E})^3} \qquad (17)$$

For H_2 in 5 N H_2SO_4 the cubic denominator term in Eq. (17) approaches 1 and

$$i \cong - \frac{{I_T}^2 \rho}{t} z^3 \phi^2 \rho \, FDC^o \ e^{-z\phi E} \qquad (18)$$

Eq. (18) thus describes a physical situation where most of the current occurs at the extreme tip of the pore adjacent to the gas phase, and power is lost by the IR drop through the remainder of the capillary, i.e. the length continuing on from the current region to the solution side. If the ℓ/t ratio is large, the resistance is high, and thus long capillaries add little to the overall performance. This effect may be seen more readily from Eq. (12). A full numerical analysis of Eq. (17) is in preparation particularly for the conditions to be used in conjunction with the experimental apparatus.

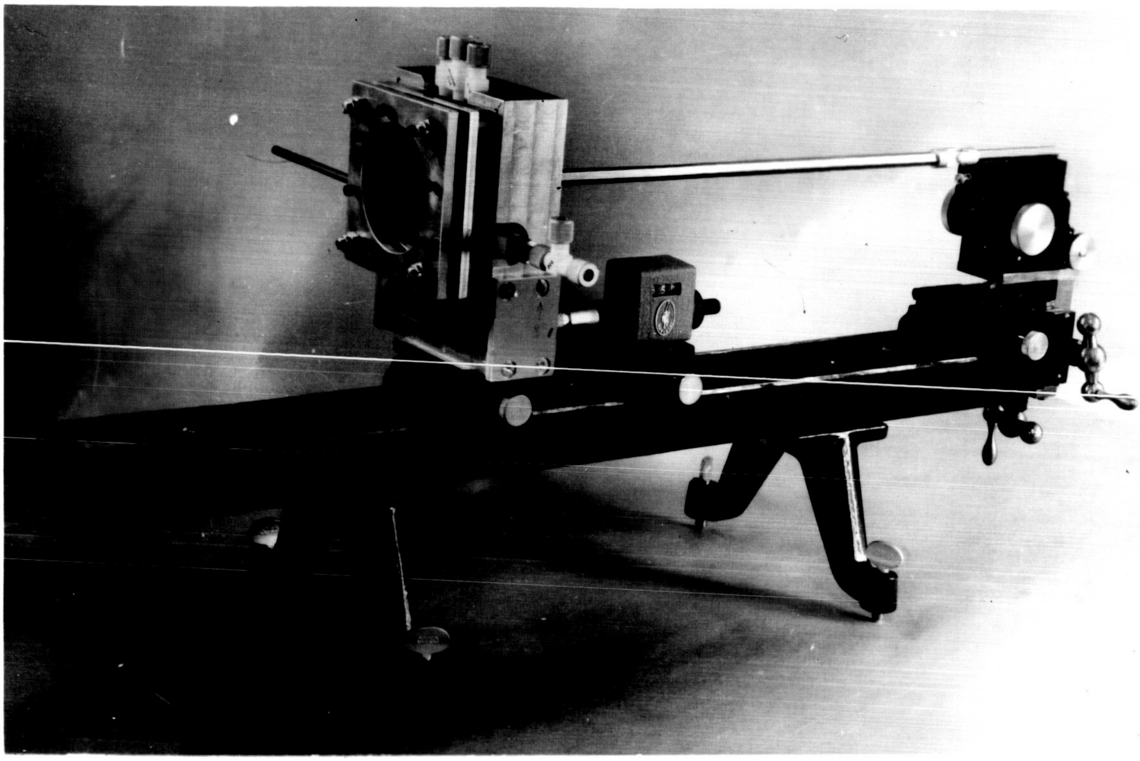

Figure 8

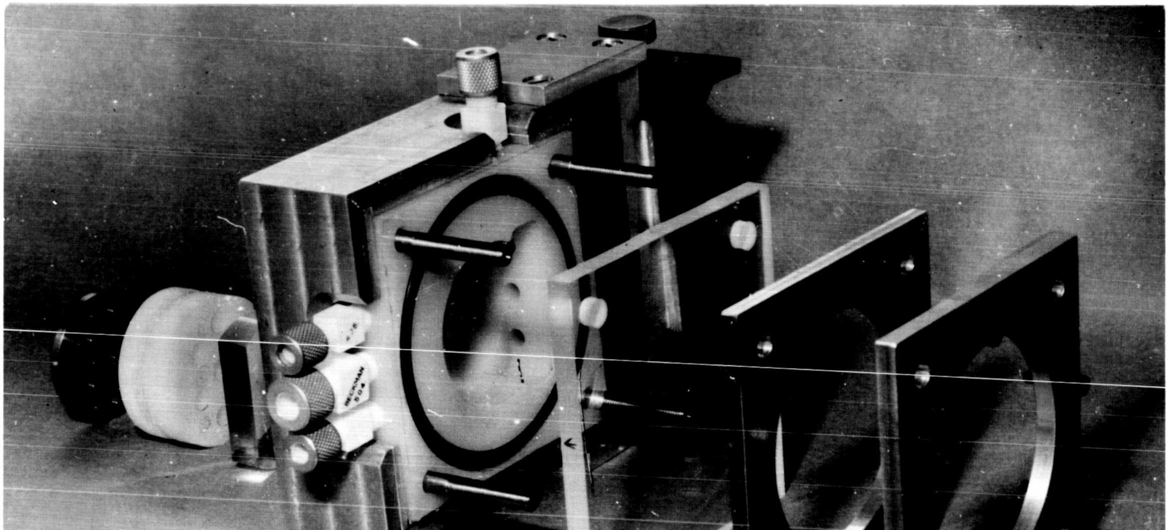

Figure 9

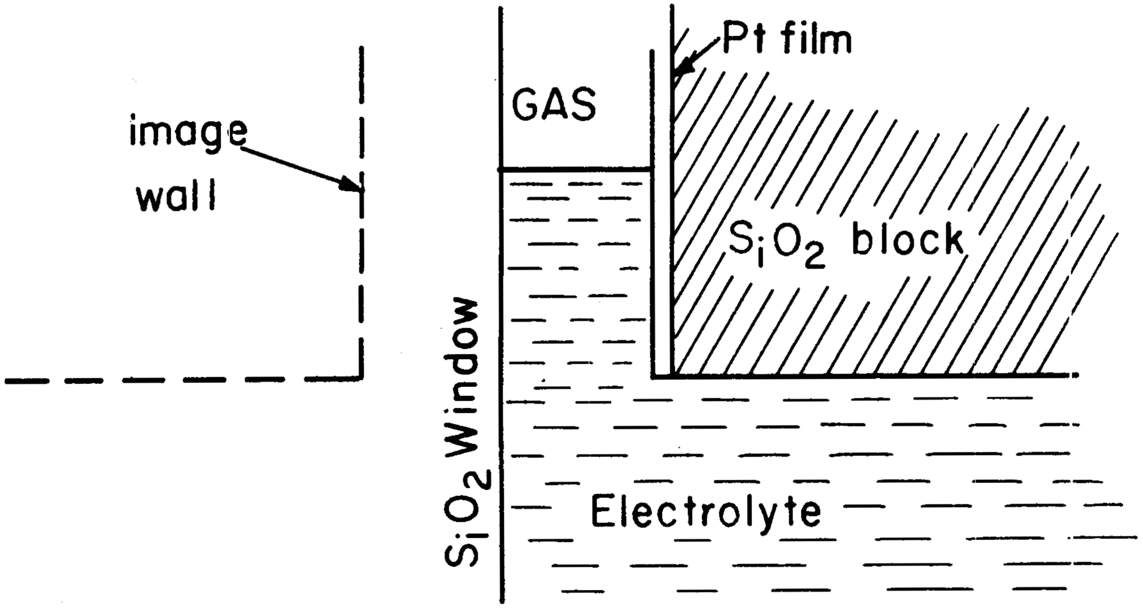
Pt film
image
wall
GAS
S_iO_2 block
S_iO_2 Window
Electrolyte

FIG. 10

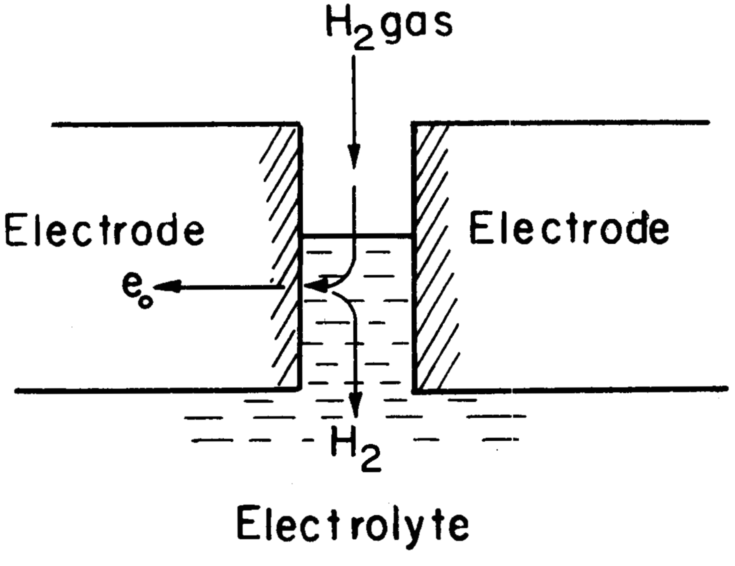
H_2gas
Electrode
Electrode
e_o
H_2
Electrolyte

FIG. 11 a

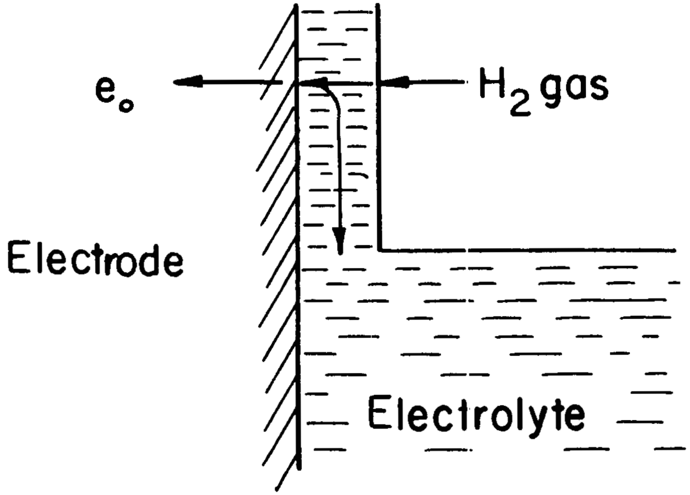
e_o
H_2gas
Electrode
Electrolyte

FIG. 11 b

THE THEORY OF ELECTRIC DOUBLE LAYERS

INTRODUCTION

In the progress report for the period 1 October 1962 - 31 March 1963, evidence was presented in favor of non-covalent bonding between a metal electrode and an ion superequivalently adsorbed on it.* Then a model, which was in the process of being developed, was described, from which the enthalpy and entropy of superequivalent adsorption (s.e.a.) were to be calculated. This non-covalent model has now been completed, and a paper has been submitted which contains the details of the model.

MODEL

In order to calculate the enthalpy of s.e.a. the following steps are carried out:

a. Firstly, n water molecules are desorbed from the electrode surface into the electrolyte, where $n = \pi r_i^2 \theta_w N_s$; r_i is the radius of the ion, θ_w is the fraction of surface sites covered by water molecules and N_s is the number of surface sites cm^{-2}. The heat of desorption is obtained from (i) the metal-water interaction, which is obtained from gaseous phase adsorption data; (ii) the lateral interaction of adsorbed water molecules, which was calculated from a previous model of water on electrodes;[3] (iii) the interaction of adsorbed water molecules with the bulk solution, which is 2 H-bonds per molecule; and (iv) the heat of

---

[*] A superequivalently adsorbed ion may be difined as one which has lost all of its hydration in the direction of the metal; i.e., no solvent molecules exist between the ion and the adsorbent surface.

condensation of water. The electrode coverage with water, θ_w, was calculated from the isotherm

$$\Delta G_{ads} - \Delta G^o_{ads} + RT \ln \frac{\theta_w}{1 - \theta_w},$$

applying the equilibrium condition, and evaluating ΔG^o_{ads} from in the aforementioned manner, used to calculate ΔH^o_{ads} (i.e., i, ii, iii, and iv). θ_w was calculated to be 0.9 with N_s being 1.3×10^{15} cm^{-2}.

b. Part of the hydration sheath must be removed from the ion in order for it to become adsorbed. The energy loss is that of ion-dipole and ion-quadrupole forces for the primary solvent molecules and Born energy (ion-dipole and ion-induced dipole interactions taken into account by the Born equation) for more distant solvent molecules.

c. The ion is placed on the electrode in the space left by the desorbed water molecules. Here it interacts with the metal with image, dispersion and repulsion forces.

d. The hole left by the ion fills with water molecules with an energy gain due to the water molecules H-bonding. Together (since the desorbed water was condensed onto the solution's surface, this term appears separately).

e. Adsorbed water molecules which are adjacent to the adsorbed ion reorient, as a result of ion interaction, and lose some adsorption energy (while gaining ion-dipole energy).

The cycle for entropy changes was given in the last report. From these motional changes for (i) the ion going to the surface; (ii) waters leaving the surface; and (iii) waters exchanging the ion, as a neighbor, for another water molecule, ΔS was calculated.

RESULTS

The calculated results for the seven ions considered are shown in Table VI. The standard state for the entropy of adsorption is taken as an ideal 1 m solution, and an ideal monolayer of adsorbed ions at half coverage. Also shown are the experimental values of $\Delta H^{o}_{s.e.a.}$ and $\Delta S^{o}_{s.e.a.}$ as obtained by Anderson and Parsons.[40] The agreement is seen to be satisfactory considering the approximate values of some of the parameters used in these calculations.

DISCUSSION OF RESULTS

From the ΔH^{o} and ΔS^{o} values of Table VI, the standard free energy of s.e.a. ($\Delta G^{o}_{s.e.a.}$) was calculated for the ions considered, and the results are shown in Table VII. Also shown are the values of s.e.a. for the various ions at the zero charge potentials in 0.1 N solutions of the ions. The calculated results predict the same order of s.e.a. as is found experimentally. Also, since ΔG^{o} is positive for the three smallest ions, the results would predict essentially no s.e.a. for them. This is in agreement with experimental facts, i.e., that ions with primary hydration sheaths are not specifically adsorbed. Lending support to the calculations is that the magnitude of differences between $\Delta G^{o}_{s.e.a.}$ for Cl^-, Br^- and I^- is nearly that predicted from experimental $q_{s.e.a.}$ values (Table VII). The bottom row in Table VII shows the calculated differences expected in ΔG^{o}, when the experimental $q_{s.e.a.}$ values are

TABLE VI

CALCULATED RESULTS OF ΔH^o AND ΔS^o OF S.E.A.

	Na^+	K^+	Cs^+	F^-	Cl^-	Br^-	I^-
Ionic Radius	0.98	1.33	1.67	1.33	1.81	1.96	2.19
Equilibrium separation of ion and metal (calc'd)	1.36	1.56	2.17	1.57	1.72	1.92	2.14
a. Desorption heat of H_2O, kcal mole^{-1}	+3.8	+7.5	+12.6	+7.5	+13.7	+16.1	+20.0
b. Hydration heat loss, kcal mole^{-1}	+42.2	+37.3	+20.6	+38.4	+23.1	+20.1	+17.0
c. Ion-metal interaction energy, kcal mole^{-1}	-49.1	-48.2	-43.5	-47.1	-49.3	-49.2	-49.2
d. Heat of filling ion vacancy with water, kcal mole^{-1}	-2.7	-3.4	02.9	-3.4	05.4	05.4	-6.1
e. Reorientation energy of primary, adsorbed waters, kcal mole^{-1}	+24.3	+13.6	+6.4	+18.7	+8.3	+5.5	±1.9
$\Delta H^o_{s.e.a.}$ (calc'd at zero coverage), kcal mole^{-1}	+18.5	+6.8	-6.8	+14.1	-9.6	-12.9	-16.4
$\Delta H^o_{s.e.a.}$ (at zero coverage) as obtained experimentally							-11.5
$\Delta S^o_{s.e.a.}$ (calc'd) in e.u. mole^{-1}	+16.3	+13.9	+1.6	+17.5	-2.1	-5.1	-11.0
$\Delta S^o_{s.e.a.}$ (as obtained experimentally) in e.u. mole^{-1}							-14.6

substituted in a Langmuir adsorption isotherm.

TABLE VII

$\Delta G^o_{s.e.a.}$ AS CALCULATED FROM MODEL

	Na^+	K^+	Cs^+	F^-	Cl^-	Br^-	I^-
s.e.a. in coul cm^{-2}	0.0	0.0	0.4	0.0	1.7	5.2	11.1
$\Delta G^o_{s.e.a.}$ in kcal $mole^{-1}$	+13.7	+2.7	-7.3	+8.9	-9.0	-11.4	-13.1
$\Delta(\Delta G^o_{s.e.a.})$ from calculations						2.4	1.7
$\Delta(\Delta G^o_{s.e.a.})$ as calc'd from exp'l results						0.6	1.4

The expected errors of the free energy calculations were analyzed. The results showed that the average uncertainty in magnitude of ΔG^o was ± 12 kcal $mole^{-1}$. These calculations also showed that the relative uncertainties in $\Delta G^o_{s.e.a.}$ could not be such as to change the order of s.e.a. amongst the various ions.

REFERENCES

1. First Semi-Annual Progress Report N.A.S.A., NS6325, 1 October 1962 - 31 March 1963.
2. M. Green, H. Dahms, J. Electrochem. Soc., 110, 466 (1963).
3. M. A. V. Devanathan, K. Müller and J. O'M. Bockris, Proc. Roy. Soc., A274, 55 (1963).
4. B. Yakuszewski and Z. Koziowski, Roczniki Chem., 36, 1873 (1962).
5. D. J. Brown, J. Coll. Sci., 13, 286 (1958).
6. R. R. Dreisbach, "P.V.T. Relationships of Organic Compounds" Handbook Publishers Inc., 1952.
7. M. Polanyi, Trans. Faraday Soc., 28, 316 (1932).
8. R. A. Pierotti and G. D. Halsey, J. Phys. Chem., 63, 680 (1959).
9. H. Wolfsohn, Z. Physik, 83, 234 (1933).
10. P. W. Selwood, "Magnetochemistry", Interscience Publishers, New York 1956.
11. A. R. Miller, Proc. Cambr. Phil. Soc., 36, 69 (1940).
12. D. A. J. Swinkels, Ph.D. Dissertation, University of Pennsylvania (1963).
13. A. F. Shepard, A. L. Henne and T. Midgeley, Jr., J. Am. Chem. Soc., 53, 1948 (1931).
14. W. M. Latimer, The Oxidation States of the Elements and their potentials in aqueous solutions, Prentice Hall, Inc., 1961.
15. V. Drazic, M. Green and J. Weber, in course of publication.
16. J. O'M. Bockris and E. Potter, J. Electrochem. Soc., 99, 169 (1952).
17. E. Lange, Miscenko, Z. Phys. Chem., 149, 1 (1930).
18. A. Frumkin, Z. Elektrochem., 59, 807 (1955).
19. E. Blomgren, J. O'M. Bockris and C. Jesch, J. phys. Chem. 65, 2000 (1961).

20. E. Blomgren, J. O'M. Bockris, J. phys. Chem. 63, 1475 (1959).

21. B. M. W. Trapnell, Chemisorption, London, Butterworths, 1955.

22. G. C. Bond, Catalysis by metals, Academic Press, London, New York, 1962.

23. A. A. Balandin, Z. Physik. Chem. B2, 289 (1929).

24. A. Sherman and H. Eyring, J. Am. Chem. Soc., 54, 2661 (1932).

25. O. H. Wansbrough-Jones, E. K. Rideal, Proc. Roy. Soc., A123, 202 (1929).

26. O. Beeck, Disc. Faraday Soc., 8, 118 (1950).

27. J. O'M. Bockris and D. A. J. Swinkels, in course of publication.
D. A. J. Swinkels, Thesis, University of Pennsylvania, 1963.

28. F. P. Bowden and L. Young, Research, 3, 235 (1950).

29. V. L. Kheifets, B. S. Krasikow, Zhur. Fr. Khim. 31, 1992 (1957).

30. G. M. Schmid, N. Hackerman, J. Electrochem. Soc., 110, 440 (1963).

31. Handbook of Chemistry and Physics, Chemical Rubber Publishing Co., 1963.

32. W. Hume-Rothery, Atomic Theory for students of metallurgy, The Institute of Metals, 1955.

33. W. Gordy, W. J. O. Thomas, J. Chem. Phys., 24, 439 (1956).

34. L. Pauling, The nature of the chemical bond, Cornell University Press, 1960.

35. J. Weber, M. Green, in course of publication.

36. H. Wroblowa, B. J. Piersma, J. O'M. Bockris, in course of publication.

37. M. L. B. Rao, M. A. V. Devanathan, J. O'M. Bockris, in course of publication.

38. Barry and Barrett, J. Am. Chem. Soc., 55, 3088 (1953).

39. C. Kemball, Proc. Roy. Soc., A190, 117 (1947).

40. W. Anderson and R. Parsons, Proc. of Second Int. Congress of Surface Activity III, p. 45, Butterworths, London (1957).